AN EXPERIMENTAL INVESTIGATION ON DNAPL MIGRATION IN SATURATED POROUS MEDIUM MODELS

Rabindra Raj GIRI[1], Takayuki UENO[2] and Kuniaki SATO[3]

[1] Student Member of JSCE, Graduate Student, Geosphere Research Institute, Saitama University, (Shimo-Okubo 255, Saitama-shi, 338-8570, Saitama, Japan).

[2] Member of JSCE, Technical Research Institute, Obayashi Corporation, (640, Shimokiyoto 4-chome, Kiyose-shi, 204-8558, Tokyo, Japan)

[3]Member of JSCE, Dr. of Eng., Professor, Geosphere Research Institute, Saitama University, (Shimo-Okubo 255, Saitama-shi, 338-8570, Saitama, Japan)

Resistance on DNAPL droplets settling in a saturated porous medium and DNAPL migration behavior through a saturated pore is experimentally investigated in this paper. Motion of a settling droplet is described by an equation, which is similar to that for a rigid solid sphere settling in an infinite liquid medium. A correlation between droplet Reynolds number (Re) and comprehensive resistance coefficient (C_R) is established for each droplet size. The results indicate that a settling droplet wobbles throughout its motion in a porous medium. Equivalent DNAPL thickness (h) in a saturated pore just before and after snap-off is correlated to pore neck area in rectangular and triangular pores. It is found that the power and linear relations hold well in the former and latter cases respectively within the data range of this study. Three different stages in DNAPL migration through a saturated pore are observed. The results indicate that the migration behavior depends on both pore geometry and DNAPL physical properties.

Key Words: *DNAPL migration, saturated porous media, comprehensive resistance coefficient, pore neck area*

1. INTRODUCTION

Soil and groundwater contamination by Dense Non-aqueous Phase Liquids (DNAPLs) is one of the major environmental problems in the industrialized world. A look into the history of DNAPL production and use reveals the major contamination in between 1950s and early 1980s. From 1980 onwards, governments, policy makers, scientists and researchers were actively engaged to prevent further contamination and remediate the contaminated sites.

DNAPL's peculiar physical properties render them highly mobile particularly in aqueous environment. A large number of literatures are available on DNAPL migration in saturated porous media. However, majority of the available literatures focused on DNAPL dissolution. Understanding pore scale phenomena is essentially important to gain knowledge on migration in macroscopic level in saturated conditions. But, the time-dependent DNAPL interfacial properties make the investigation of pore scale phenomena more complicated[1].

J.G. Roof investigated snap-off mechanism for oil droplets through water saturated circular pores on theoretical and experimental basis[2]. An experimental study on generation and snap-off of DNAPL droplets through water saturated triangular pores reported that the snap-off height and snapped droplet size depend on both DNAPL properties and pore geometry[3]. Some authors demonstrated correlation among pore size, DNAPL droplet size, and resistance to motion of a settling droplet in saturated uniform porous midium[4].

The uncertainties involved in investigating pore scale phenomena due to temporal variation in DNAPL interfacial properties could be one of the reasons for smaller numbers of literatures available on this topic. However, the knowledge of pore scale processes based on average interfacial properties is

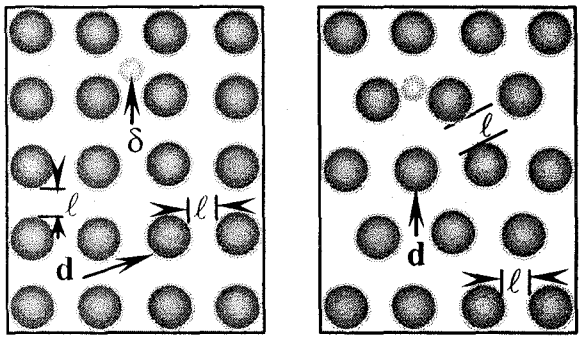

(a) (b)

Fig. 1 Schematic diagram of porous media in experiment - I: (a) model - 1 and (b) model - 2

essentially useful in understanding the migration and other related phenomena in the saturated subsurface.

The objectives of this paper are to understand (a) settlement behavior of a DNAPL droplet in porous media and (b) characteristics of DNAPL migration through a pore in water saturated condition. Two experimental investigations are carried out to achieve these objectives that are termed as experiment I and II respectively as discussed in the following sections. Dyed trichloroethylene (TCE) and perchloroethylene (PCE) are used as representative DNAPLs. The experiments are carried out in a constant temperature (25^0C) and humidity (50%) room.

2. EQUATION FOR A DNAPL DROPLET SETTLEMENT (EXPERIMENT-I)

The motion of a rigid spherical solid settling in a stagnant infinite liquid medium is expressed by the following equation.

$$\frac{\partial U}{\partial t} = \left(\frac{\rho_s - \rho_\ell}{\rho_s}\right) g - C_D \frac{3\rho_\ell U^2}{4\delta\rho_s} \qquad (1)$$

where, C_D = drag coefficient, U = settling velocity of the solid, δ = diameter of the sphere, and ρ_s and ρ_ℓ = densities for solid sphere and liquid medium respectively. Unlike a rigid sphere in infinite liquid medium, the shape of a DNAPL droplet settling in a saturated porous medium changes depending on various resistance forces that are specifically unknown. However, the motion can be approximated by equation (1) taking additional resistance effects due to many unknown reasons into account. In this experiment, the resultant effect of various resistance forces on the droplet is termed as comprehensive resistance coefficient (C_R) and δ represents equivalent diameter of the deformed droplet. Assuming the time-averaged droplet velocities as steady and taking all the resistance

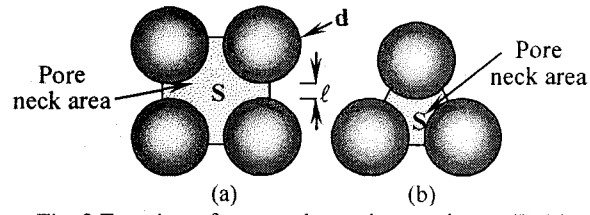

(a) (b)

Fig. 2 Top view of pore neck area in experiment -II: (a) rectangular pore and (b) triangular pore

effects into account, C_R for a DNAPL droplet settling through water saturated stagnant porous medium can be expressed in the following form[5].

$$C_R = \frac{4g\delta^3}{3\rho_\ell \mathrm{Re}^2 \nu^2}\left(\frac{\rho_d - \rho_\ell}{\rho_\ell}\right) \qquad (2)$$

where, $\mathrm{Re} = U_0\delta/\nu$ = droplet Reynolds number, ρ_d = DNAPL density, ν = kinematic viscosity for water and U_0 = time averaged droplet velocity in the porous medium.

In this experiment, the droplet Reynolds number and comprehensive resistance coefficient for a DNAPL droplet settling through a saturated porous medium are correlated by equation (2). The extent of droplet deformation is commonly expressed in terms of dimensionless numbers. In literatures, both Weber number and Eotvos number are commonly used as independent variables for correlating shape parameters for fluid particles[6]. However, Eotvos number gives a better overall representation, which is expressed as follows.

$$E_0 = \frac{g\delta^2(\rho_d - \rho_\ell)}{\sigma} \qquad (3)$$

where, σ = interfacial tension for DNAPL.

Two types of porous media are used in this experiment that are designated as model-1 and model-2 as depicted in **Fig. 1**.

3. DNAPL MIGRATION BEHAVIOR IN A SATURATED PORE (EXPERIMENT-II)

DNAPL physical properties and pore geometry could be two main factors that govern its migration through water saturated pore. In addition, solid surface characteristics, wetting phase liquid properties and temperature may play significant roles. Temperature changes have appreciable effects on DNAPL physical properties. Temporal variation in DNAPL interfacial properties may impose uncertainties on an accurate assessment of its migration behavior through a saturated pore. There could be several forces that act on DNAPL body in migration process. But, there are no such theories and mathematical expressions to describe the migration behavior probably due to the above

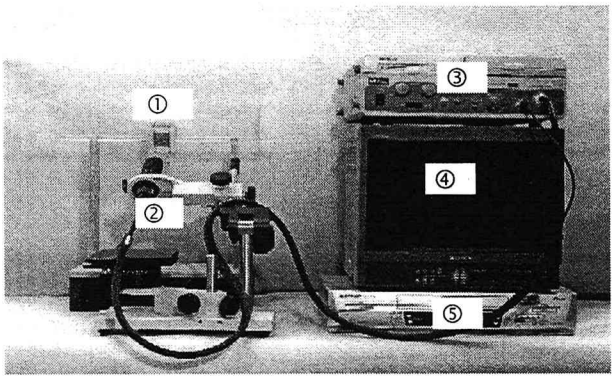

① = Porous medium, ② = Microscope camera, ③ = Microscope body, ④ = Video monitor and ⑤ = Video recorder

Fig. 3 A view of the experimental set-up

mentioned uncertainties. In this experiment, our attempt is to illuminate on this behavior in general, and correlate migration volume with pore geometry and DNAPL density neglecting the temporal changes in their interfacial properties.

4. EXPERIMENTAL SET-UP AND PROCEDURE

A photographic view of the experimental set-up used in the study is depicted in **Fig. 3**. In experiment-I, a digital camera replaces the microscope camera. The porous media consist of uniform glass spheres (5-mm diameter) placed between two transparent glass plates (6.0 cm × 12.0 cm) as depicted in **Fig. 1**. The clearance between two adjacent spheres (ℓ), TCE droplet sizes (δ), and relative clearance values (ℓ/δ) used in the experiment are shown in **Table 1**. After clamping a saturated model in a vertical rigid support, a TCE droplet is released from the top of a pore in the model and its motion through the pore is video recorded. The procedure is repeated for every combination of the selected clearance values and droplet sizes. Average droplet settling velocities are then calculated by displaying the video records. Droplet Reynolds number, Eotvos number and values of comprehensive resistance coefficient are calculated based on the average settling velocities using equations shown in the previous section. These parameters are computed for droplets settling in infinite liquid medium also to compare the values with that in porous media.

In experiment-II, the pore models consist of uniform glass sphere placed on a horizontal plane and saturated with water as shown in **Fig. 2**. Rectangular and triangular pores with and without clearance between them are considered in this case. The clearance is denoted by ℓ, which are given two values (0 and 1-mm). The glass sphere sizes and corresponding pore sizes in this experiment are shown in **Table 2.** DNAPL is gradually poured into the pore with the help of an injection syringe. As pouring is continued, it moves down through the pore resulting to bulging beneath the pore neck. The bulging goes on increasing and finally a portion gets detached from the DNAPL body. This is known as snap-off phenomenon. The total DNAPL volumes in the pore just before and after the snap-off are recorded carefully. The ratio of the DNAPL volumes at these two instances (V) and pore neck area (S) is termed as equivalent DNAPL thickness in the pore and is denoted by "h".

Table 1 Cases in experiment - I

S.N.	(ℓ) mm	ℓ/δ ratio for droplet diameter (δ) mm					
		1.99	2.32	2.47	2.87	3.25	3.85
1.	7	3.52	3.02	2.83	2.44	2.15	1.82
2.	6	3.02	2.57	2.43	2.09	1.85	1.56
3.	5	2.51	2.15	2.02	1.74	1.54	1.29
4.	4	2.01	1.72	1.63	1.39	1.23	1.04
5.	3	1.51	1.29	1.21	1.04	0.92	0.78

Table 2 Cases in experiment - II

Glass sphere dia. (d) mm	Pore neck space (mm^2)			
	Rectangular pore		Triangular pore	
	$\ell = 0$	$\ell = 1$	$\ell = 0$	$\ell = 1$
2.0	-	5.86	-	-
3.0	1.93	8.93	-	3.39
3.5	2.63	10.63	-	-
4.0	3.43	12.43	-	4.54
5.0	5.36	16.36	1.01	5.77
6.0	7.72	20.73	1.45	7.08
7.0	10.52	-	1.97	8.47
10.5	-	-	4.44	-
12.5	-	-	6.30	-

5. RESULTS AND DISCUSSIONS

(1) Experiment - I

A DNAPL droplet released from the top of vertical pore experiences various resistances resulting in its wobbling motion. A TCE droplet, as observed in the experiments, collides with the solid spheres and bounces to different directions. In some instances, it gets stuck with the solids. The deformations in droplet shape depend on ℓ/δ ratio.

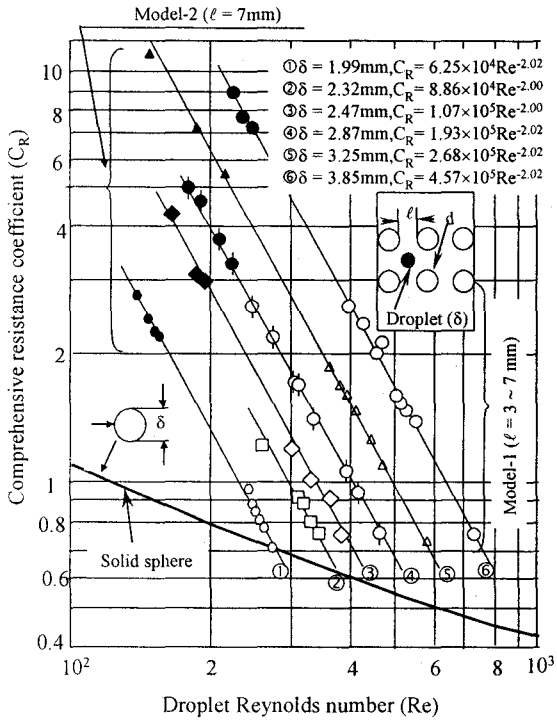

Fig. 4 Relationship between Re and C_R

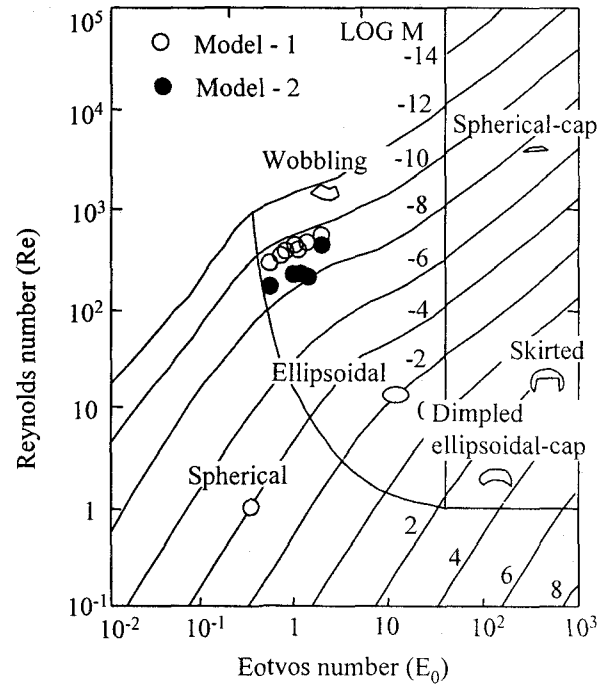

Fig. 5 Relationship between Re and E_0

For smaller ratios, the motion resembles to plug flow to some extent in model-1. Majority of the droplets is broken after collision with solid spheres in model-2.

Fig. 4 shows relationships between droplet Reynolds number and comprehensive resistance coefficient. The thick solid line is for a rigid sphere settling in an infinite liquid medium. The functional relationships between these two parameters (C_R and Re) for TCE droplets are shown in the same figure. As depicted in the figure, the relation for each droplet size is almost a straight line in log-log graph. The bottom most point in each line represents the result for infinite liquid medium condition. The points towards the top left-hand side (solid) are for model-2, whereas the remaining points are for model-1. All the points for TCE droplets lie above the line for a solid sphere in infinite liquid medium. The results for smaller droplet size in infinite liquid medium are very close to the line for solid sphere. As the droplet diameter increases, the point moves away from the line. For the selected range of TCE droplet sizes and clearance (ℓ) values in this experiment, the droplet Reynolds number and comprehensive resistance coefficient vary in between 100 to 1000 and 0.7 to 11.0 respectively.

The functional relationships between these two parameters for each droplet size, as shown in the **Fig. 4**, can be expressed by the following equation.

$$C_R = \alpha\, Re^{-n} \qquad (4)$$

where, α ranges from 6.25×10^4 to 4.57×10^5 and the exponent (n) has almost constant value of 2.0 in the present study.

Clift et al.[6] have presented a generalized shape diagram for fluid bubbles and droplets rising/settling in stagnant infinite liquid medium as depicted in **Fig. 5**. It is a relation between particle Reynolds number and Eotvos number, which is commonly used in estimating shape regimes of fluid particles. The results of the present experiments fall in the wobbling region of the diagram. Droplet deformation increases with increasing droplet size. However, there is no such significant difference between model-1 and model-2 with respect to droplet deformation.

It is evident from these results that smaller DNAPL droplets behave similar to solid spheres in stagnant infinite liquid medium. As the droplet size increases, it deviates from the idealized solid sphere case and deformations in shape increase comprehensive resistance coefficient values. These values further increase due to the presence of solid particles in porous media. ℓ/δ ratio is a key parameter to describe a droplet motion behavior in this study. As this ratio decreases, the average droplet velocity decreases resulting to decrease in droplet Reynolds number and hence increase in comprehensive resistance coefficient in both models. However, more frequent collisions of settling droplets with solid particles in model-2 makes its travel path longer resulting to smaller

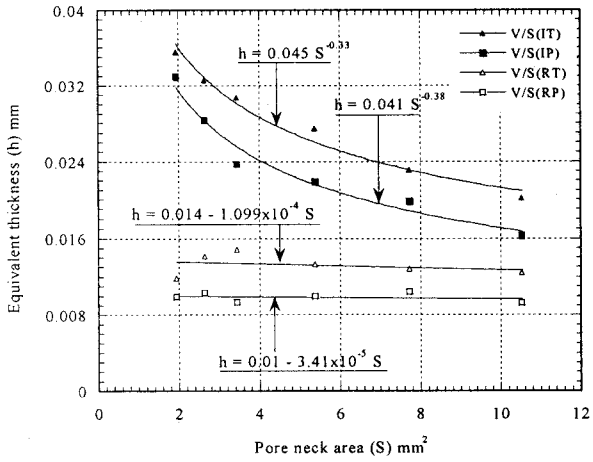

Fig. 6 Relation between h and S for rectangular pore ($\ell = 0$)

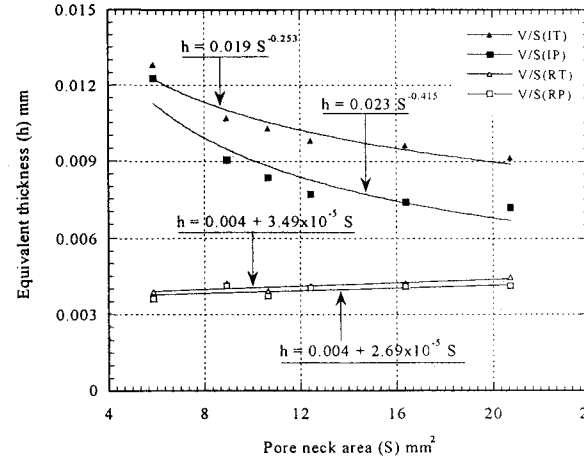

Fig. 7 Relation between h and S for rectangular pore ($\ell = 1$)

average velocity and hence smaller values of droplet Reynolds number and increase in comprehensive resistance coefficient.

(2) Experiment - II

DNAPL volume held in a saturated pore depends on DNAPL interfacial properties, pore geometry and surface characteristics of solid particles in the porous medium. But, very little is known about the influence of these factors separately. So, assessing the influence of solid particles' surface characteristics and temporal changes in DNAPL interfacial properties is beyond the scope of this study. Only the effects of pore geometry, and physical properties (mainly density in this case) for two typical DNAPLs (TCE and PCE) are discussed here.

Fig. 6 and **7** show relationships between equivalent DNAPL thickness (h) and S for 0-mm and 1-mm clearances (ℓ) respectively in rectangular pores. Power and linear laws respectively best approximate the relations for total DNAPL volume in the pores just before and after snap-off, as depicted in the figures. In the legends of the figures, I = initial or total DNAPL volume in a pore just before snap-off, R = residual volume after snap-off, T = TCE and P = PCE.

The effect of DNAPL density difference can be clearly observed for the case just before snap-off, where PCE has exhibited smaller volumes and h values. But, the effect of density is not significant for residual volume in ℓ = 1-mm case. In the beginning when pore space increases from its smaller values, h decreases quickly in power law relations. As the pore space further increases, the rate of decrease in h value slows down. This tendency is clearly observed in ℓ = 0-mm case. The curves for ℓ = 1-mm case are relatively flat. In the case of residual volume, it appears from the figures that h has almost constant values for smaller pore space, where as it seems to increase as pore neck space increases within the range of the present experiment.

The results of the triangular pores are presented in **Fig. 8** and **9** for ℓ = 0-mm and 1-mm cases respectively. The tendencies are similar to that for rectangular pores. However, the power law curves are steeper for ℓ = 0-mm case compared to that of the rectangular case probably due to smaller pore neck areas. The gradients of the curves for residual DNAPL volume also seem bigger than for the corresponding cases in rectangular pores. Smaller pores do not exhibit significant effect of DNAPL density difference on penetration volume. As the pore space increases, it becomes significant in both types of pores for the total volume just before snap-off. In case of residual volume, it does not show appreciable effect.

As discussed briefly in the earlier section based on the experimental observations, three distinct cases of DNAPL penetration through a water-saturated pore are observed. For smaller pore spaces, DNAPL volume in a pore behaves like a deformed droplet. Interfacial tension force seems to be predominant to other forces. This behavior is frequently observed in smaller triangular pores. As the pore neck area increases, a droplet like behavior no longer exists. The DNAPL volume covers the neck space and forms a film. The film thickness decreases as the pore space increases. In the third stage as the pore space is further increased, the DNAPL volume moves down the sides of the pore before covering the entire neck space to form a film. In this case, gravitational force could be dominant in comparison to interfacial tension and other resistance forces. In general, it can be inferred based on the results that pores with no clearance between the adjacent spheres can retain bigger

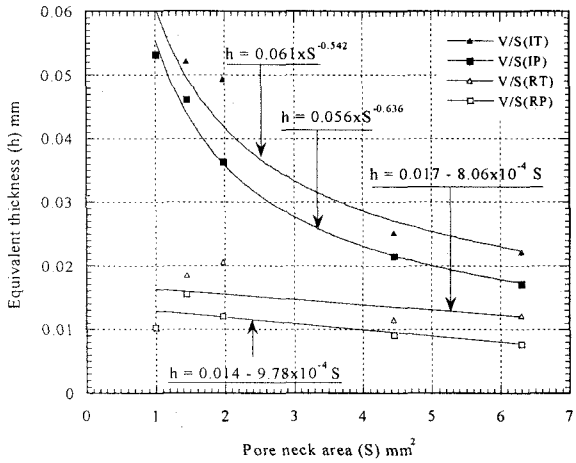

Fig. 8 Relation between h and S for triangular pore ($\ell = 0$)

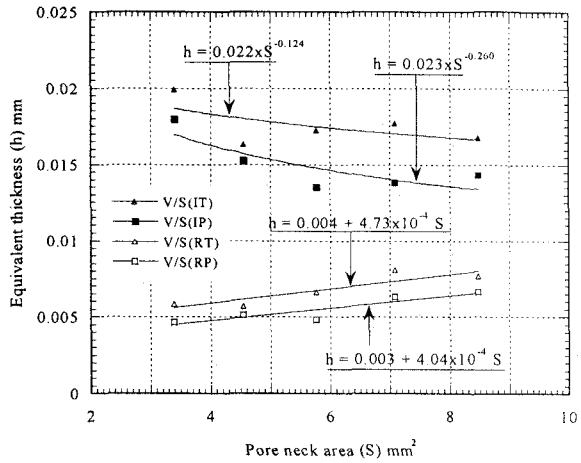

Fig. 9 Relation between h and S for triangular pore ($\ell = 1$)

DNAPL volume compared to 1-mm clearance case, probably because the former offers relatively higher resistance effect to downward migration. Similarly, triangular pores can do so compared to rectangular one probably due to the same reason.

The power and linear relationships between h and S for both types of pores can be expressed by the following general equations.

$$h = a\,S^{-b} \qquad (5)$$

$$h = p + qS \qquad (6)$$

where, a, b, p and q are constants. The numerical values for them vary from 1.9×10^{-2} to 6.1×10^{-2}, 12.4×10^{-2} to 6.36×10^{-2}, 3.0×10^{-3} to 1.7×10^{-2} and -3.41×10^{-5} to 4.73×10^{-4} respectively in the present experimental study.

6. CONCLUSION

Settlement of a DNAPL droplet through water saturated porous media and DNAPL migration behavior in saturated pores is experimentally investigated in this study. The motion of a settling DNAPL droplet in a saturated porous medium is approximated by an equation similar to that for a solid sphere settling in an infinite liquid medium. The comprehensive resistance coefficient (C_R) is correlated with droplet Reynolds number (Re). Power law (equation-4) expresses the correlation for different droplet sizes. The results reveal that the comprehensive resistance coefficient varies between 0.7 and 11.0 corresponding to the droplet Reynolds number variation between 100 and 1000 for the droplet sizes and ℓ/δ ratios considered in the study. The results also indicate that a settling droplet wobbles throughout its motion in saturated porous media.

The results of DNAPL migration through a water saturated pore indicate that the relation between equivalent DNAPL thickness just before snap-off and pore neck space can be best approximated by power law within the range of the present experimental conditions. A linear equation best describes the relationship for residual volume after snap-off. DNAPL migration behavior through a saturated pore depends on both pore geometry and DNAPL properties. Three distinct phases of penetration are observed in the present study.

REFERENCES

1) David, M.T.: Time-dependent interfacial properties and DNAPL mobility, *Westinghouse Savannah River Co.*, Savannah River Technology Center, USA, pp.1-9, March 1999.
2) Roof, J.G.: Snap-off of oil droplets in water-wet pores, *Society of Petroleum Engineers Journal*, pp.85-90, March, 1970.
3) Hung, V.D., Sato, K. and Imamura, S.: Generation of dense non-aqueous phase liquid drops in saturated porous media, *J. of Groundwater Hydrology*, Vol. 40(3), pp.289-310, 1998.
4) Hung, V.D., Sato, K. and Imamura, S.: Hydraulic resistance exerted on dense non-aqueous phase liquid droplets moving through saturated porous media, *the 27th IAHR Congress*, 1997.
5) Ueno, T., Giri, R.R. and Sato, K.: Resistance on DNAPL droplet settlement through saturated porous medium models, *the 29th IAHR Congress*, Beijing, Sept. 2001.
6) Clift, R. and Weber, M.E.: *Bubbles, Drops and Particles*, Academic Press, Inc., pp. 23-28, 169-174, 1978.
7) Ueno, T., Giri, R.R. and Sato, K.: Modeling of DNAPL penetration processes through saturated porous medium, Symposium on Flow Modeling and Turbulence Measurement (FMTM), Tokyo (Japan), Dec. 2001.
8) Conrad, S.H., Wilson, J.L., Mason, W.R. and Peplinski, W.J.: Visualization of residual organic liquid trapped in aquifers, *Water Resources Research*, Vol. 28(2), pp.467-478, 1992.
9) Oostrom, M., Hofstee, C., Walker, R.C. and Dane, J.H.: Movement and remediation of trichloroethylene in saturated heterogeneous porous medium, 1: Spill behaviors and initial dissolution, *J. of Contaminant Hydrology*, Vol. 37, pp. 159-178, 1999.

(Received October 1, 2001)